

Superconducting gap induced barrier enhancement in a BiFeO₃-based heterostructure

C. L. Lu,^{1,2} Y. Wang,² L. You,² X. Zhou,² H. Y. Peng,¹ G. Z. Xing,¹ E. E. M. Chia,¹ C. Panagopoulos,¹ L. Chen,² J.-M. Liu,^{3,4} J. Wang,^{2,a)} and T. Wu^{1,b)}

¹*Division of Physics and Applied Physics, School of Physical and Mathematical Sciences, Nanyang Technological University, Singapore 637371*

²*School of Materials Science and Engineering, Nanyang Technological University, Singapore 639798*

³*Laboratory of Solid State Microstructure, Nanjing University, Nanjing 210093, People's Republic of China*

⁴*International Center for Materials Physics, Chinese Academy of Science, Shenyang 110016, People's Republic of China*

(Received 17 November 2010; accepted 2 December 2010; published online 23 December 2010)

We report the synthesis and characterization of an epitaxial heterostructure composed of multiferroic BiFeO₃ and superconducting YBa₂Cu₃O_{7-δ} thin films grown on (001) SrTiO₃. Both the superconductivity of YBa₂Cu₃O_{7-δ} and the ferroelectricity of BiFeO₃ are retained in the heterostructure. Current density-electric field characteristics measured from 30 to 170 K suggest a Schottky-emission-like transport at the BiFeO₃/YBa₂Cu₃O_{7-δ} interface. Furthermore, the temperature dependence of the barrier height shows an anomalous enhancement at T_C , indicating an intimate coupling between the multiferroic and the superconducting layers. © 2010 American Institute of Physics. [doi:10.1063/1.3530446]

Multiferroics, materials simultaneously exhibiting multiple ferroic orders, have attracted significant attention due to the fundamental science and the tantalizing technological perspective.¹⁻⁴ BiFeO₃ (BFO) is one of the most studied multiferroic materials because of its room temperature lead-free ferroelectricity ($T_C \sim 1103$ K) and antiferromagnetism ($T_N \sim 643$ K).⁵⁻⁷ At room temperature bulk BFO has a rhombohedral structure (point group $R3c$) with lattice parameters $a = 5.6343$ Å and $\alpha_r = 59.348^\circ$.⁸ Its spontaneous polarization ($P \sim 100$ μC/cm²) along the pseudocubic $\langle 111 \rangle$ directions originates from the high stereochemical activity of Bi lone pairs,⁹ and could be the biggest switchable polarization among all perovskite ferroelectrics. The Fe³⁺ spins are responsible for the G-type antiferromagnetic (AFM) ordering.^{4,9,10} Recently, reorientation of the easy M planes accompanying the P switching has been demonstrated by Zhao *et al.*¹¹ using photoemission electron microscopy. Such a strong correlation between P and M , along with other exotic phenomena such as the electric field controlled exchange bias and the giant tunnel magnetoresistance, has inspired researchers to explore various BFO-based heterostructures.¹²⁻¹⁵

In this work, we report the synthesis and characterization of a multiferroic/superconductor heterostructure composed of BFO and YBa₂Cu₃O_{7-δ} (YBCO) thin films. Interfacial couplings in such heterostructures can potentially present a wide range of emergent phenomena.¹⁶ Indeed, a variety of fascinating properties has been evidenced in YBCO-based junctions,¹⁷⁻²¹ rendering the BFO/YBCO heterostructure an excellent candidate in the search for novel properties in low dimensions.

The thin film heterostructures of BFO and YBCO were grown using pulsed laser deposition (PLD) on (001) SrTiO₃

(STO) single crystal substrates with TiO₂ surface termination. High quality YBCO thin film with good crystallinity and superconductivity was usually obtained at high substrate temperatures, *e.g.*, ~ 800 °C,^{17,22} which may degrade BFO.^{23,24} Therefore, YBCO was deposited first, which also served as the bottom electrode in ferroelectric (FE) and transport studies. The YBCO bottom layer with a thickness of ~ 80 nm was grown in 150 mTorr oxygen at a substrate temperature of 780 °C, and then the BFO thin film was deposited at 80 mTorr and 670 °C. The topographic imaging and the piezoresponse force microscopy (PFM) measurements were carried out on an atomic force microscope (Asylum Research, USA, MFP-3D). Ferroelectric hysteresis loops were obtained using a precision ferroelectric tester (Radiant Technologies, USA). The temperature dependent dielectric property and the current density-electric field (J - E) curves were measured in a Janis Research cryogenic probe-station equipped with a Keithley 4200 semiconductor characterization system (Keithley, USA).

The x-ray diffraction (XRD) spectra for both the YBCO thin film and the BFO/YBCO heterostructure are shown in Figs. 1(a) and 1(b). The pure c -axis orientation indicates good crystallinity and epitaxial growth on the STO (001) substrate. No impurity phase was detected in the heterostructure, indicating negligible interdiffusion or reaction at the interface. The out-of-plane lattice parameter of BFO in the heterostructure was found to be 3.99 Å, which is larger than that of the bulk counterpart (3.96 Å), indicating a biaxial compressive strain. This is in agreement with previous reports of BFO grown on STO substrates.^{4,5}

As shown in the topographic image in Fig. 1(c), the YBCO surface is covered by uniform nanoscale islands with a root mean square roughness (R_{rms}) of ~ 2.3 nm. The observed surface morphology has been reported previously for YBCO thin films due to the strain relaxation during deposition,²² which makes the subsequent deposition of high quality BFO a challenge.²³⁻²⁶ To probe the superconducting

^{a)} Author to whom correspondence should be addressed. Electronic mail: jlwang@ntu.edu.sg.

^{b)} Electronic mail: tomwu@ntu.edu.sg.

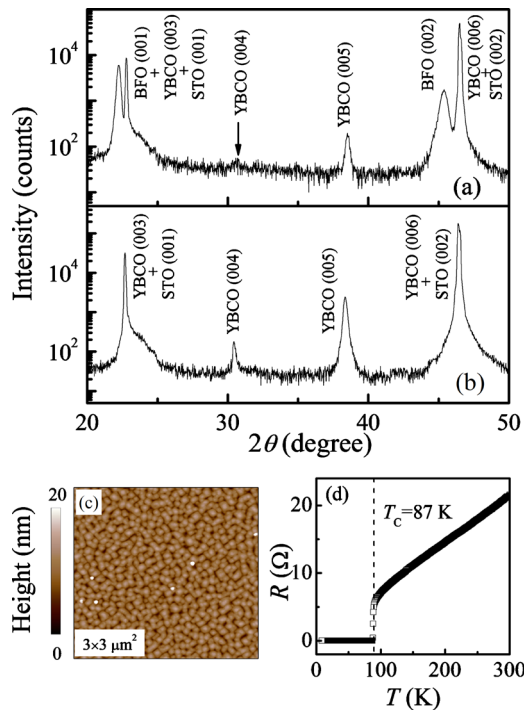


FIG. 1. (Color online) XRD patterns of (a) BFO/YBCO/STO and (b) YBCO/STO thin films. (c) $3 \times 3 \mu\text{m}^2$ topographic AFM image and (d) resistance vs temperature measured on the YBCO/STO thin film. The superconducting transition is indicated by a dashed line in (d).

properties of the heterostructure, we measured the T -dependence of resistance under zero magnetic field, and Fig. 1(d) depicts the onset of superconductivity at $T_C = 87$ K.^{17–20}

After depositing BFO (~ 350 nm), the top surface of the heterostructure becomes rougher with an increased R_{rms} of ~ 23 nm. The corresponding topographic image in Fig. 2(a) shows grains larger than those on the single YBCO layer. The out-of-plane PFM image is depicted in Fig. 2(b), which was recorded simultaneously with the topographic scan. Yellow (bright) and purple (dark) contrasts in Fig. 2(b) represent spontaneous polarization component pointing “up” and “down,” respectively. Most importantly, ferroelectricity was retained in the BFO/YBCO thin film heterostructure as evidenced in the FE hysteresis loops in Fig. 2(c) measured at different temperatures. The FE loops are squarelike with large remanent polarization P_r of 65 – $70 \mu\text{C}/\text{cm}^2$, which agrees well with previous reports.⁴ For comparison, BFO thin films were also grown on the conventionally used SrRuO₃ (SRO) buffer layers under the same growth conditions, and the corresponding FE loop [the solid line in Fig. 2(c)] is similar to the BFO/YBCO case. The quality of samples was further confirmed by the ε - E curves [Fig. 2(d)] measured at different temperatures showing the typical double-loop feature with two peaks appearing at the coercive field.

Accompanying the room temperature multiferroic properties, a well-known problem of BFO thin films is the large leakage current,^{27–30} leading to relatively high dielectric losses. The J - E curves of the Pt/BFO/YBCO capacitorlike heterostructures were measured from room temperature down to 30 K. The FE domains were poled before each measurement. Figure 3 depicts typical transport data which

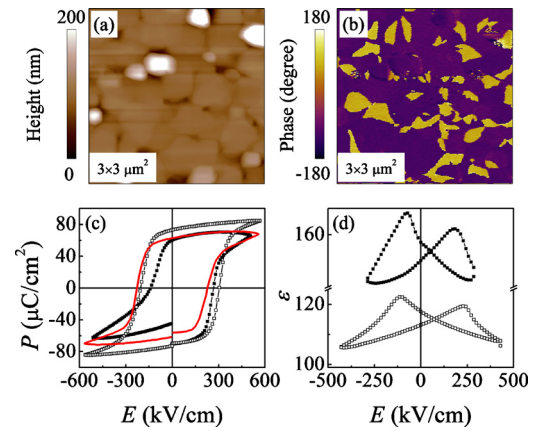


FIG. 2. (Color online) (a) $3 \times 3 \mu\text{m}^2$ topographic AFM image of the BFO thin film grown on YBCO/STO. (b) Corresponding piezoresponse phase image. Yellow (bright) and purple (dark) correspond to the original up and down domains, respectively. Electric field dependence of (c) the spontaneous polarization and (d) the dielectric constant measured at 300 (solid squares) and 77 K (open squares). For comparison, the room temperature P - E loop (solid line) of the BFO thin film deposited on a SrRuO₃ buffer layer is also shown in (c).

contain some key information about this multiferroics/superconductor heterostructure.

Most recently, it has been demonstrated that the leakage current of Pt/BFO/SrRuO₃ (SRO) capacitor is interface-limited.²⁷ Considering that YBCO is also an oxide electrode like SRO, we assumed that the same interface-limited mechanism dominates in the present Pt/BFO/YBCO heterostructures. Indeed, extensive fittings to the transport data suggest that the Schottky-like barrier model is most suitable to describe the conduction behavior observed in our samples. The current density across a Schottky barrier is³¹

$$J = AT^2 \exp - \left[\frac{\Phi}{k_B T} - \frac{1}{k_B T} \left(\frac{q^3 V}{4\pi\epsilon_0 K d} \right)^{1/2} \right],$$

where A is the Richardson constant, k_B is the Boltzmann constant, q is the electron charge, Φ is the Schottky barrier height (SBH), K is the optical dielectric constant, and d is the sample thickness. Typical fitting results at five different temperatures are shown in Fig. 3(a) (the solid curves of the negative branches). The fitting ranges are uniformly fixed. From the fitting, we estimate the optical dielectric constant K

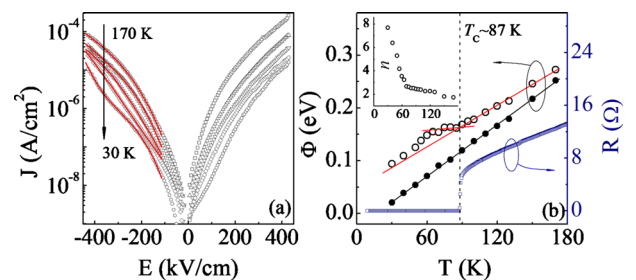


FIG. 3. (Color online) (a) Typical J - E characteristics of the Pt/BFO/YBCO heterostructure measured at various temperatures (only 170, 150, 110, 80, and 30 K data are shown for clarity). The solid curves of the negative branches represent the corresponding fitting results using the Schottky-like barrier model. (b) Schottky barrier height Φ as a function of temperature (open circles), along with the T -dependent resistance of YBCO (open squares). The lines are the linear fittings, and the dot line marks the superconducting transition. Inset in (b) is the T -dependent refractive index n deduced from fitting. For comparison, $\Phi(T)$ data of the Pt/BFO/SRO junction are also shown (solid circles), and the black line is guide for eyes.

and the barrier height Φ . To reveal the effect of the superconducting transition on the BFO/YBCO interface, we plotted the T -dependence of Φ [Fig. 3(b)]. Interestingly, a clear steplike anomaly of $\Phi(T)$ was observed at $T_C=87$ K. After subtracting the linear background, the deviation of SBH was estimated to be ~ 19 meV which is close to the superconducting gap of ~ 30 – 60 meV in YBCO,^{17,18,20} while their difference warrants further investigations. Similar SBH anomalies, caused by the evolution of the superconducting gap, have been previously observed in other superconductor-based junctions.^{18,32} Actually, the current Pt-BFO-YBCO structure can be modeled as two Schottky-like diodes with a back-to-back configuration, which would contribute to the transport behavior simultaneously. To exclude the possibility that the observed steplike anomaly of $\Phi(T)$ might originate from the Pt/BFO interface, we also carried out similar measurements on the Pt/BFO/SRO junction, and the absence of the $\Phi(T)$ anomaly in that case as shown in Fig. 3(b) further confirms that the anomaly in the Pt/BFO/YBCO case originates from the superconducting transition of YBCO.

The optical refractive index n can be deduced from the optical dielectric constant K through the relation of $n=K^{1/2}$, and its comparison with the ideal value of about 2.5–3.1 can be used to evaluate the validity of fitting.^{27–30} The T -dependence of n is shown in the inset of Fig. 3(b). Upon cooling to 65 K, n increases within the range of 1.73–3.21. This is close to the expected values, indicating that the Schottky emission dictates the conduction in the BFO/YBCO heterostructures at $T \geq 65$ K. Further cooling causes a rapid increase of n , becoming much larger than the ideal value, which suggests that the Schottky emission plays a less important role at the low temperatures.

In conclusion, high quality c -axis oriented epitaxial BFO/YBCO thin film heterostructures were fabricated on SrTiO₃ (100) substrate and shown to retain ferroelectricity and superconductivity. The transport behaviors of the BFO/YBCO interface measured at different temperatures can be well described using the Schottky-like barrier model. Furthermore, a steplike anomaly was observed in the temperature-dependent barrier height data, which are associated with the evolution of the superconducting gap in YBCO. These results may encourage future studies on other multiferroic/superconductor heterostructures to explore the interactions across the interfaces and to construct advanced devices with tunable functionalities.

This work was supported by the Singapore National Research Foundation and the Ministry of Education of Singapore (Grant Nos. AcRF RG30/06, ARC 23/08, and ARC 16/08). J.-M. Liu was supported by NSFC (Grant Nos. 50832002 and 10874085).

¹S.-W. Cheong and M. Mostovoy, *Nature Mater.* **6**, 13 (2007).

²K. F. Wang, J.-M. Liu, and Z. F. Ren, *Adv. Phys.* **58**, 321 (2009).

³T. Choi, S. Lee, Y. J. Choi, V. Kiryukhin, and S.-W. Cheong, *Science* **324**, 63 (2009).

⁴G. Catalan and J. F. Scott, *Adv. Mater.* **21**, 2463 (2009); S. A. T. Redfern, C. Wang, J. W. Hong, G. Catalan, and J. F. Scott, *J. Phys.: Condens. Matter* **20**, 452205 (2008).

⁵J. Wang, J. B. Neaton, H. Zheng, V. Nagarajan, S. B. Ogale, B. Liu, D. Viehland, V. Vaithyanathan, D. G. Schlom, U. V. Waghmare, N. A. Spaldin, K. M. Rabe, M. Wuttig, and R. Ramesh, *Science* **299**, 1719 (2003).

⁶R. Palai, R. S. Katiyar, H. Schmid, P. Tissot, S. J. Clark, J. Robertson, S. A. T. Redfern, G. Catalan, and J. F. Scott, *Phys. Rev. B* **77**, 014110 (2008).

⁷D. C. Arnold, K. S. Knight, F. D. Morrison, and P. Lightfoot, *Phys. Rev. Lett.* **102**, 027602 (2009).

⁸F. Kubel and H. Schmid, *Acta Crystallogr., Sect. B: Struct. Sci.* **46**, 698 (1990).

⁹N. A. Hill, *J. Phys. Chem. B* **104**, 6694 (2000); M. K. Singh, R. S. Katiyar, and J. F. Scott, *J. Phys.: Condens. Matter* **20**, 252203 (2008).

¹⁰D. Lebeugle, D. Colson, A. Forget, M. Viret, A. M. Bataille, and A. Gukasov, *Phys. Rev. Lett.* **100**, 227602 (2008).

¹¹T. Zhao, A. Scholl, F. Zavaliche, K. Lee, M. Barry, A. Doran, M. P. Cruz, Y. H. Chu, C. Ederer, N. A. Spaldin, R. R. Das, D. M. Kim, S. H. Beak, C. B. Eom, and R. Ramesh, *Nature Mater.* **5**, 823 (2006).

¹²Y.-H. Chu, L. W. Martin, M. S. Holcomb, M. Gajek, S.-J. Han, Q. He, N. Balke, C.-H. Yang, D. Lee, W. Hu, Q. Zhan, P.-L. Yang, A. F. Rodríguez, A. Scholl, S. X. Wang, and R. Ramesh, *Nature Mater.* **7**, 478 (2008).

¹³L. W. Martin, Y.-H. Chu, M. B. Holcomb, M. Huijben, P. Yu, S. J. Han, D. Lee, S. X. Wang, and R. Ramesh, *Nano Lett.* **8**, 2050 (2008).

¹⁴H. Béa, M. Bibes, S. Cherifi, F. Nolting, B. W. Fonrose, S. Fusil, G. Herranz, C. Deranlot, E. Jacquet, K. Bouzehouane, and A. Barthélémy, *Appl. Phys. Lett.* **89**, 242114 (2006).

¹⁵H. Béa, M. Bibes, M. Sirena, G. Herranz, K. Bouzehouane, E. Jacquet, S. Fusil, P. Paruch, M. Dawber, J.-P. Contour, and A. Barthélémy, *Appl. Phys. Lett.* **88**, 062502 (2006).

¹⁶J. Y. Gu, C.-Y. You, J. S. Jiang, J. Pearson, Ya. B. Bazaliy, and S. D. Bader, *Phys. Rev. Lett.* **89**, 267001 (2002).

¹⁷W. Ramadan, S. B. Ogale, S. Dhar, L. F. Fu, S. R. Shinde, D. C. Kundaliya, M. S. R. Rao, N. D. Browning, and T. Venkatesan, *Phys. Rev. B* **72**, 205333 (2005).

¹⁸J. R. Sun, C. M. Xiong, Y. Z. Zhang, and B. G. Shen, *Appl. Phys. Lett.* **87**, 222501 (2005).

¹⁹R. Ramesh, A. Inam, W. K. Chan, F. Tillerot, B. Wilkens, C. C. Chang, T. Sands, J. M. Tarascon, and V. G. Keramidis, *Appl. Phys. Lett.* **59**, 3542 (1991).

²⁰H. J. Zhang, X. P. Zhang, J. P. Shi, and Y. G. Zhao, *J. Phys. D: Appl. Phys.* **41**, 135110 (2008); H. J. Zhang, X. P. Zhang, J. P. Shi, H. F. Tian, and Y. G. Zhao, *Appl. Phys. Lett.* **94**, 092111 (2009).

²¹C. H. Ahn, J.-M. Triscone, and J. Mannhart, *Nature (London)* **424**, 1015 (2003).

²²B. Dam, J. M. Huijbregste, and J. H. Rector, *Phys. Rev. B* **65**, 064528 (2002).

²³L. You, N. T. Chua, K. Yao, L. Chen, and J. L. Wang, *Phys. Rev. B* **80**, 024105 (2009).

²⁴H. Béa, M. Bibes, A. Barthélémy, K. Bouzehouane, E. Jacquet, A. Khodan, J.-P. Contour, S. Fusil, F. Wyczisk, A. Forget, D. Lebeugle, D. Colson, and M. Viret, *Appl. Phys. Lett.* **87**, 072508 (2005).

²⁵Y. H. Chu, Q. He, C. H. Yang, P. Yu, L. W. Martin, P. Shafer, and R. Ramesh, *Nano Lett.* **9**, 1726 (2009).

²⁶Y. H. Chu, Q. Zhan, L. W. Martin, M. P. Cruz, P. L. Yang, G. W. Pabst, F. Zavaliche, S. Y. Yang, J. X. Zhang, L. Q. Chen, D. G. Schlom, I.-N. Lin, T.-B. Wu, and R. Ramesh, *Adv. Mater.* **18**, 2307 (2006).

²⁷L. Pintilie, C. Dragoi, Y. H. Chu, L. W. Martin, R. Ramesh, and M. Alexe, *Appl. Phys. Lett.* **94**, 232902 (2009).

²⁸G. W. Pabst, L. W. Martin, Y. H. Chu, and R. Ramesh, *Appl. Phys. Lett.* **90**, 072902 (2007).

²⁹H. Yang, M. Jain, N. A. Suvorova, H. Zhou, H. M. Luo, D. M. Feldmann, P. C. Dowden, R. F. Depaula, S. R. Foltyn, and Q. X. Jia, *Appl. Phys. Lett.* **91**, 072911 (2007).

³⁰G. L. Yuan and J. L. Wang, *Appl. Phys. Lett.* **95**, 252904 (2009).

³¹W. Schottky, *Naturwiss.* **26**, 843 (1938).

³²C. T. Wu, H. H. Chang, J. Y. Luo, T. J. Chen, F. C. Hsu, T. K. Chen, M. J. Wang, and M. K. Wu, *Appl. Phys. Lett.* **96**, 122506 (2010).